

Determining the Unknown Traction of a Cracked Elastic Body Using the Inverse Technique with the Dual Boundary Element Method

Ru-Min Chao, Yen-Ji Chen and F.C. Lin¹

Abstract: The two-dimensional elasticity problem of an isotropic material, containing a *centered-crack* with unknown boundary traction is studied by the inverse procedure. The dual boundary integral equations are used to analyze the problem. While solving the ill-posed inverse problem, both of the conjugate gradient method and the regularization method are used. A scaling factor depending upon the material constant μ is introduced into the sensitivity matrix in order to keep the order of magnitude the same throughout the formulation. The result by using the displacement measurement will be compared with those by stress measurement, and an extensive discussion will be given. Finally, the effect of measurement error to the inverse problem is also discussed.

keyword: Inverse Problem, Crack, Dual Boundary Integral Equation, Regularization Method, Conjugate Gradient Method, Displacement, Stress, Measurement Error.

1 Introduction

Boundary element methods and inverse problems have been called attentions by many researchers in the field of science and engineering. In the elasticity problem, Gao and Mura(1989) used the surface displacement to determine the residual stress field around the damaged area. Yeih, Koya and Mura(1993) showed the theoretical approach of the inverse elasticity problem with partially overprescribed boundary conditions. On the second part of their paper, Koya, Yeih and Mura(1993) gave some numerical results. For more inverse problems related to structural mechanics can be referred to Kubo(1988). Recently, a book given by Ingham and Wrobel(1997) collects several articles showing the inverse analysis by boundary integral formulation could be applied to several fields of engineering. Chen and Hong(1999) also gave an

extensive review for the applications by the dual boundary element methods.

Inverse elasticity problems containing cracks are seldom to see in the literature, and most of them are flaw detection problems. Mellings and Aliabadi(1995) studied the flaw identification problem of an elastic body using either the internal or the boundary displacement/stress sensors. More recently, Huang and Shih(1999) studied the multiple crack identification in an elastic body, but whose analysis was restricted to symmetric loading conditions, and only the internal displacement measurement was used.

If crack appears in a structure, the internal stress has been re-distributed if compared with the previous un-cracked system. To access the fatigue life of such a structure requires comprehensive knowledge of the boundary conditions surrounding the crack. Directly measuring the boundary information in this case is not easy because the structure detail might be constructed by welding of plate, girder and stiffener.

This paper is devoted to the two-dimensional inverse elastic crack problem with unknown boundary traction. By studying this problem, eventually we would like to establish a framework of solving the unknown traction problem of a complex marine structure for practical use. The displacement discontinuous method (DDM) derived from the dual boundary integral equation by Mi(1996), Hong and Chen(1988) is used. We use the discontinuous quadratic boundary elements for modeling the crack surfaces, and the continuous quadratic elements for the rest of the boundary. The readers can refer Hong and Chen (1988) for the basics of the dual boundary integral equations in the elasticity problem, and Portela and Aliabadi(1992) for the numerical implementation of the method. Information at selected internal sensor points is calculated by the direct analysis, which is used to represent the experimental measurement data in the inverse analysis. The influence of random distribution of mea-

¹ National Cheng Kung University, Dept. of Naval Architecture and Marine Engineering, Tainan, Taiwan 701 R.O.C
Email:rmchao@mail.ncku.edu.tw

surement error is also discussed in this study.

While solving the ill-posed inverse problem, both of the conjugate gradient method, (see Huang and Shih(1997)) and the regularization method (see Maniatty and Zabaras(1994)) are used. Due to the inconsistent order of the magnitude of the fundamental solutions within the dual boundary integral equations, a scaling factor at the order of μ is introduced to the sensitivity matrix, and the inverse solution is very accurate. In general, the iterative conjugate gradient method requires more computational time than the regularization method to reach the final solution. It is found that, within a large range of the regularization parameter, the regularization method will result in a more accurate inverse solution. This enables us to have a one-shot regularization solution, which is good enough for the final estimation.

Numerical experiments show that using the internal stress information will result in a better inverse solution than those by using the internal displacement data. The influence due to different sensor locations and crack size is also studied.

2 The Dual Integral Equations

The boundary integral equations for the two-dimensional linear elastic problem are given in any standard text books, that is, Brebbia and Dominguez(1992), Becker(1992). Neglecting the body force, in an isotropic and homogeneous elastic solid, the relation between the displacement u_k and the traction t_k can be expressed in terms of the following integral equation,

$$C_{lk}(x')u_k(x') = \int_{\Gamma} U_{lk}(x',x)t_k(x) d\Gamma(x) - \text{CPV} \int_{\Gamma} T_{lk}(x',x)u_k(x) d\Gamma(x) \quad (1)$$

where Γ denotes the entire boundary of the solid, x' represents the field point, x is a point on the Γ , and CPV stands for the Cauchy principal-value of the integral. The U_{lk} and the T_{lk} are the fundamental solutions of the displacement and the traction, respectively, also are known as the Kelvin's solution. Let Ω denote the domain in consideration, the constant $C_{lk}(x')$ can be calculated indirectly by utilizing the rigid body motion. In general, it is defined as the following:

$$C_{lk}(x') = \begin{cases} \delta_{lk} & (x' \in \Omega) \\ \delta_{lk}/2 & (x' \in \text{on smooth boundary}) \\ 0 & (x' \notin \Omega) \end{cases}$$

The stress component σ_{ij} at an internal point X' is given by

$$\sigma_{ij}(X') = \int_{\Gamma} D_{kij}(X',x)t_k(x) d\Gamma(x) - \int_{\Gamma} S_{kij}(X',x)u_k(x) d\Gamma(x) \quad (2)$$

where $S_{kij}(X',x)$ and $D_{kij}(X',x)$ are linear combinations of the derivatives of $T_{ij}(X',x)$ and $U_{ij}(X',x)$, respectively. Equations (1) and (2) constitute the basis of the dual boundary element method, see also in Hong and Chen(1988), Portela(1993).

Let $\Gamma = \Gamma_e + \Gamma_+ + \Gamma_-$, where Γ_e represents the external boundary, Γ_+ and Γ_- are the upper and the lower crack surfaces, respectively. Considers a point, x^+ locating on top of the crack surfaces. Since there is another point, x^- sharing the same coordinates on the opposite crack surface, the displacement boundary integral equation at the point, x^+ can be modified as

$$\frac{1}{2}u_k(x^+) + \frac{1}{2}u_k(x^-) = \int_{\Gamma} U_{lk}(x^+,x) d\Gamma(x) - \text{CPV} \int_{\Gamma} T_{lk}(x^+,x)u_k(x) d\Gamma(x) \quad (3)$$

The traction boundary integral equation at x^- is rewritten as

$$\frac{1}{2}t_j(x^-) - \frac{1}{2}t_j(x^+) = n_j(x^-)\text{CPV} \int_{\Gamma} D_{kij}(x^-,x)t_k(x) d\Gamma(x) - n_j(x^-)\text{HPV} \int_{\Gamma} S_{kij}(x^-,x)u_k(x) d\Gamma(x) \quad (4)$$

where HPV stands for the Hadamard principal value of the integral, and n_i denotes the i th component of the unit outward normal vector at the boundary point x' . Over the crack surface, it is found that $T_{ij}(x^+,x) = T_{ij}(x^-,x)$ and the direction on the crack contour is opposite for the upper and the lower surfaces, i.e., $\Gamma_+ = -\Gamma_-$. Therefore, by defining the displacement discontinuous function $\Delta u_j(x) = u_j(x^+) - u_j(x^-)$, the traction boundary in-

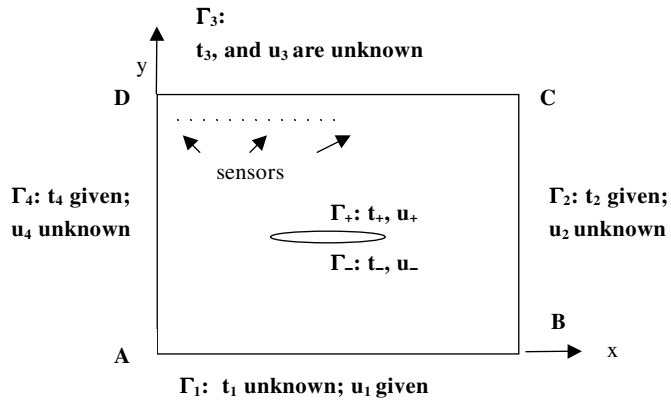


Figure 1 : Statement of the inverse elasticity problem.

tegral equation, (4) can be rewritten as

$$\begin{aligned}
 n_i(x^-) \int_{\Gamma_e} D_{kij}(x^-, x) t_k(x) d\Gamma(x) = \\
 n_i(x^-) \int_{\Gamma_e} S_{kij}(x^-, x) u_k(x) d\Gamma(x) \\
 + n_i(x^-) HPV \int_{\Gamma_+} S_{kij}(x^-, x) \Delta u_k(x) d\Gamma(x) \quad (5)
 \end{aligned}$$

by assuming that traction is free on crack surface.

The displacement discontinuous function is identified as the crack opening displacement (COD) as in the fracture mechanics, and the use of equation (1) and (5) is usually refer to the displacement discontinuity method (DDM). The reader can also refer to Hong and Chen(1988) and Mi(1996) for more details of the displacement discontinuity method.

3 The Direct Problem

To discuss the direct problem, let us again consider a two-dimensional plate with a crack at its center, see Fig. 1. The boundary Γ is divided into five sub-boundaries, i.e., $\Gamma = \Gamma_1 + \Gamma_2 + \Gamma_3 + \Gamma_4 + \Gamma_5$, where $\Gamma_e = \Gamma_1 + \Gamma_2 + \Gamma_3 + \Gamma_4$ represents the external boundaries and $\Gamma_5 = \Gamma_+ + \Gamma_-$ represents the crack contour. To discretize the outer boundaries into boundary elements, the displacement boundary integral equation (1) is used with the continuous quadratic boundary elements. Without loss of generality, it enables us to write the system of linear algebraic equation as

$$\mathbf{HU} = \mathbf{GT} \quad (6)$$

where $\mathbf{U} = \{(u)_1, (u)_2, (u)_3, (u)_4, (\Delta u)_5\}^T$ represents the vector of displacement at the boundary nodes, and $(u)_i$ is the displacement vector associated with the sub-boundary;

$\mathbf{T} = \{(t)_1, (t)_2, (t)_3, (t)_4, (t)_5\}^T$ represents the vector of traction at the boundary nodes, and $(t)_i$ is the traction vector associated with the sub-boundary;

\mathbf{H}, \mathbf{G} = geometry dependent matrices containing integration of weakly and strongly singular kernel of U_{ij} , and T_{ij} , and the subscripts of $[H]_{ij}$, $[G]_{ij}$ represent the influence of the boundary value on sub-boundary i by the boundary value on sub-boundary, j , i.e.,

$$\mathbf{H} = \begin{bmatrix} [H]_{11} & [H]_{12} & [H]_{13} & [H]_{14} & [H]_{15} \\ [H]_{21} & [H]_{22} & [H]_{23} & [H]_{24} & [H]_{25} \\ [H]_{31} & [H]_{32} & [H]_{33} & [H]_{34} & [H]_{35} \\ [H]_{41} & [H]_{42} & [H]_{43} & [H]_{44} & [H]_{45} \end{bmatrix} \quad (7)$$

and

$$\mathbf{G} = \begin{bmatrix} [G]_{11} & [G]_{12} & [G]_{13} & [G]_{14} & [G]_{15} \\ [G]_{21} & [G]_{22} & [G]_{23} & [G]_{24} & [G]_{25} \\ [G]_{31} & [G]_{32} & [G]_{33} & [G]_{34} & [G]_{35} \\ [G]_{41} & [G]_{42} & [G]_{43} & [G]_{44} & [G]_{45} \end{bmatrix} \quad (8)$$

For the DDM method, the discretization form of (5) is

$$\mathbf{H}'\mathbf{U} = \mathbf{G}'\mathbf{T} \quad (9)$$

where \mathbf{H}' and \mathbf{G}' are geometry dependent matrices containing integration of the strongly singular and the hyper-singular kernel of S_{kij} , and D_{kij} . That is

$$\mathbf{H}' = [[H]_{51} [H]_{52} [H]_{53} [H]_{54} [H]_{55}] \quad (10)$$

and

$$\mathbf{G}' = [[G]_{51} [G]_{52} [G]_{53} [G]_{54} [G]_{55}] \quad (11)$$

If the boundary conditions are well defined, equation (6) and (9) are combined, and the final linear algebraic equations can be solved by any standard numerical procedure. Then the displacement at any internal point can be calculated according to (1), and in terms of the matrix form

$$\mathbf{U}'' = \mathbf{G}''\mathbf{T} - \mathbf{H}''\mathbf{U} \quad (12)$$

where \mathbf{U}'' = vector of the displacement at the internal points;

$\mathbf{H}'', \mathbf{G}''$ = matrices depending on internal points with regular type of integration.

The stress component at the internal points can also calculated from equation (2), that is

$$\mathbf{S} = \mathbf{G}'''\mathbf{T} - \mathbf{H}'''\mathbf{U} \quad (13)$$

where \mathbf{S} is the vector of stress components at the internal points, \mathbf{H}''' and \mathbf{G}''' are matrices depending on internal points with regular type of integration.

4 The Inverse Problem

In inverse analysis, the boundary conditions over Γ_3 in Fig. 1 are assumed fully unknown, and they are determined with the help from the measured information at the sensor points. The rest of boundaries are specified with either the displacement or the traction condition.

If the sensor readings are the displacement data, that is

$$\mathbf{u}(\bar{\mathbf{x}}) = \mathbf{Y}_{\text{measured}}(\bar{\mathbf{x}}), \text{ where } \bar{\mathbf{x}} \text{ is in } \Omega \quad (14)$$

where $\mathbf{u}(\bar{\mathbf{x}})$ represents the displacement information for all of the internal sensor points in the x and in the y direction. The inverse problem becomes to utilize the measurement information, $\mathbf{Y}_{\text{measured}}(\bar{\mathbf{x}})$, then to estimate the unknown boundary traction, t_3 on Γ_3 , where

$$\mathbf{Y}_{\text{measured}} = (Y_{x,\text{measured}}, Y_{y,\text{measured}}).$$

The solution of the present inverse problem is obtained in such a way that the following functional by minimizing:

$$\mathbf{J}(t|_{\Gamma_3}) = \sum_{i=1}^N [(u_{x,\text{estimated}}^i - Y_{x,\text{measured}}^i)^2 + (u_{y,\text{estimated}}^i - Y_{y,\text{measured}}^i)^2] \quad (15)$$

where $\mathbf{u}^i = (u_{x,\text{estimated}}^i, u_{y,\text{estimated}}^i)$ denotes the estimated displacement information in the x and the y directions at the sensor point, the superscript $i=1, N$ represents the identification number of the sensor, and N is the total number of sensors being selected. During the numerical experiment, the estimated displacement data is determined from the direct problem by using the estimated boundary traction on the boundary Γ_3 .

Regarding the \mathbf{U}'' in equation (12) as the measured displacement at the sensors, Koya, Yeh and Mura(1993), Pasquetti and Petit(1995) combine equations (6), (9) and (12) to give the following linear system of equations as:

$$\begin{bmatrix} \mathbf{H} \\ \mathbf{H}' \\ \mathbf{H}'' \end{bmatrix} \mathbf{U} = \begin{bmatrix} \mathbf{G} \\ \mathbf{G}' \\ \mathbf{G}'' \end{bmatrix} \mathbf{T} + \begin{bmatrix} 0 \\ 0 \\ -\mathbf{U}'' \end{bmatrix} \quad (16)$$

The above equation contains all of the unknowns on the boundaries and the measuring data at the sensors, thus it gives a larger linear system of equations than the direct problem. Rearranging all the unknowns in a vector \mathbf{X} leads to the following equation:

$$\mathbf{A}\mathbf{X} = \mathbf{B} \quad (17)$$

Since the iterative conjugate gradient method suggested by Kammerer and Nashed(1972) requires a symmetric, positive definite matrix. The above equation is then multiplied by \mathbf{A}^T , and one gets

$$\mathbf{A}^T\mathbf{A}\mathbf{X} = \mathbf{A}^T\mathbf{B} \quad (18)$$

Here \mathbf{A} is the sensitivity matrix and \mathbf{X} is a column vector containing all of the unknown conditions on the boundaries. In our case, $\mathbf{X} = \{t_1, u_2, u_3, u_4, \Delta u_5, t_3\}$.

For some of the engineers, it is more intuitive to use the stress measurement data instead of the displacement measurement data, because the stress measurement is much more convenient to get. If the sensor readings are stress components at the sensor point, that is

$$S(\bar{\mathbf{x}}) = Y_{\text{measured}}(\bar{\mathbf{x}}), \quad (19)$$

where $\bar{\mathbf{x}}$ is in Ω , and $S(\bar{\mathbf{x}})$ represents the normal and the shear stress measuring information for all of the internal sensor points. The inverse problem becomes to utilize the stress measurement information, $\mathbf{Y}_{\text{measured}}(\bar{\mathbf{x}})$, then to estimate the unknown boundary traction, t_3 on Γ_3 . In this case, $\mathbf{Y}_{\text{measured}} = (\sigma_{xx,\text{measured}}, \sigma_{yy,\text{measured}}, \sigma_{xy,\text{measured}})$.

The solution of the inverse problem using stress measurement information is obtained in such a way that the following functional is minimized:

$$\mathbf{J}(t|_{\Gamma_3}) = \sum_{i=1}^N \left[\left(\sigma_{xx,\text{estimated}}^i - \sigma_{xx,\text{measured}}^i \right)^2 + \left(\sigma_{yy,\text{estimated}}^i - \sigma_{yy,\text{measured}}^i \right)^2 + \left(\sigma_{xy,\text{estimated}}^i - \sigma_{xy,\text{measured}}^i \right)^2 \right] \quad (20)$$

where $\sigma^i = (\sigma_{xx,\text{estimated}}^i, \sigma_{yy,\text{estimated}}^i, \sigma_{xy,\text{estimated}}^i)$ denotes the estimated normal and shear stresses at the sensor point. These quantities are determined by equation (13) with the estimated boundary traction on the boundary Γ_3 . Eventually, the inverse analysis becomes to solve

the following linear system of equations:

$$\begin{bmatrix} \mathbf{H} \\ \mathbf{H}' \\ \mathbf{H}''' \end{bmatrix} \mathbf{U} = \begin{bmatrix} \mathbf{G} \\ \mathbf{G}' \\ \mathbf{G}''' \end{bmatrix} \mathbf{T} + \begin{bmatrix} 0 \\ 0 \\ -\mathbf{S} \end{bmatrix} \quad (21)$$

Rearranging the above equation in a form like (17), the inverse problem using the internal stress measurement is solved.

5 Numerical Methods

It is understood that, the entities of the matrices $[\mathbf{H}]$ and $[\mathbf{G}]$ are calculated by integrating the fundamental solutions with the order of magnitude $O(1)$ and $O(1/\mu)$, respectively. Notice that μ is the shear modulus of the material. However, the entities of the matrices $[\mathbf{H}']$ and $[\mathbf{G}']$ are $O(\mu)$ and $O(1)$, respectively. We therefore introduce the scaling factor of μ into equation (16) and (21) in order to have a uniform order of magnitude in the sensitivity matrix. The following equations are adopted for the subsequent analysis:

$$\begin{bmatrix} \mathbf{H} \\ \mathbf{H}'/\mu \\ \mathbf{H}'' \end{bmatrix} \{\mu\mathbf{U}\} = \begin{bmatrix} \mu\mathbf{G} \\ \mathbf{G}' \\ \mu\mathbf{G}'' \end{bmatrix} \{\mathbf{T}\} + \begin{bmatrix} 0 \\ 0 \\ -\mu\mathbf{U}'' \end{bmatrix} \quad (22)$$

for the inverse analysis using the displacement measurement data, and

$$\begin{bmatrix} \mathbf{H} \\ \mathbf{H}'/\mu \\ \mathbf{H}'''/\mu \end{bmatrix} \{\mu\mathbf{U}\} = \begin{bmatrix} \mu\mathbf{G} \\ \mathbf{G}' \\ \mathbf{G}''' \end{bmatrix} \{\mathbf{T}\} + \begin{bmatrix} 0 \\ 0 \\ -\mathbf{S} \end{bmatrix} \quad (23)$$

for the inverse analysis using the stress measurement data.

5.1 The Conjugate Gradient Method

The conjugate gradient method described in Kammerer and Nashed(1972), and Huang and Shih(1997) is first used to solve the linear system of equations (18). A quick review of the iterative conjugate gradient method will be described as in Fig. 2. Both of the displacement and the stress measurements will be used as the sensor information in the inverse analysis.

The stopping criterion for the iterative conjugate gradient method requires the functional, \mathbf{J} to satisfy the following equation

$$\mathbf{J}(\mathbf{t}|_{\Gamma_3}) < \varepsilon \quad (24)$$

and ε is a small number.

5.2 The Regularization Method

The regularization method is a modification of the sum of square function with the addition of the regularization terms, and these additional terms have a smoothing effect on the unknown function components, see Maniatty and Zabaraz (1994). The following system of equations are solved by the Gaussian elimination method with partially pivoting for the unknown boundary traction:

$$(\mathbf{A}^T \mathbf{A} + \alpha \mathbf{D}^T \mathbf{D}) \mathbf{X} = \mathbf{A}^T \mathbf{B} \quad (25)$$

where \mathbf{D} is the zero-th order regularization square matrix which is defined as

$$\mathbf{D} = \begin{bmatrix} 1 & 0 & \cdots & 0 \\ 0 & 1 & \cdots & 0 \\ 0 & 0 & \ddots & 0 \\ 0 & \cdots & 0 & 1 \end{bmatrix} \quad (26)$$

and α is the regularization parameter.

For the regularization method in used, the selection of the regularization parameter is the crucial subject to the accuracy of the inverse solution. During our numerical experiments, α is first chosen to be 10^{-1} while solving the problem, and it will be ten times smaller for the next calculation until equation (24) is satisfied. If (24) is always violated, then the secant search method will be provided to find the solution for the minimum of \mathbf{J} .

5.3 The Error Analysis

For the inverse analysis, we simply perform a numerical experiment whose measured information comes from the direct (exact) solution. In order to compare the results due to the randomly distributed measurement error, 1 percent of the measurement average is assumed to be the standard deviation of the experimental error. If the measurement error follows the normal distribution, uncorrelated with zero mean and constant standard deviation, then the measured information can be expressed as

$$Y_{measured} = Y_{exact} + \lambda \bar{\sigma}, \quad (27)$$

where Y_{exact} is the solution from the direct problem; $\bar{\sigma}$ is the standard deviation of the measurement error, and λ is a random number in the range of $(-2.576, 2.576)$, which can be generated by an IMSL library named DRNNOR. Thus, the experiment measurement data of 99% confidence will be fallen in this interval according to equation (27)

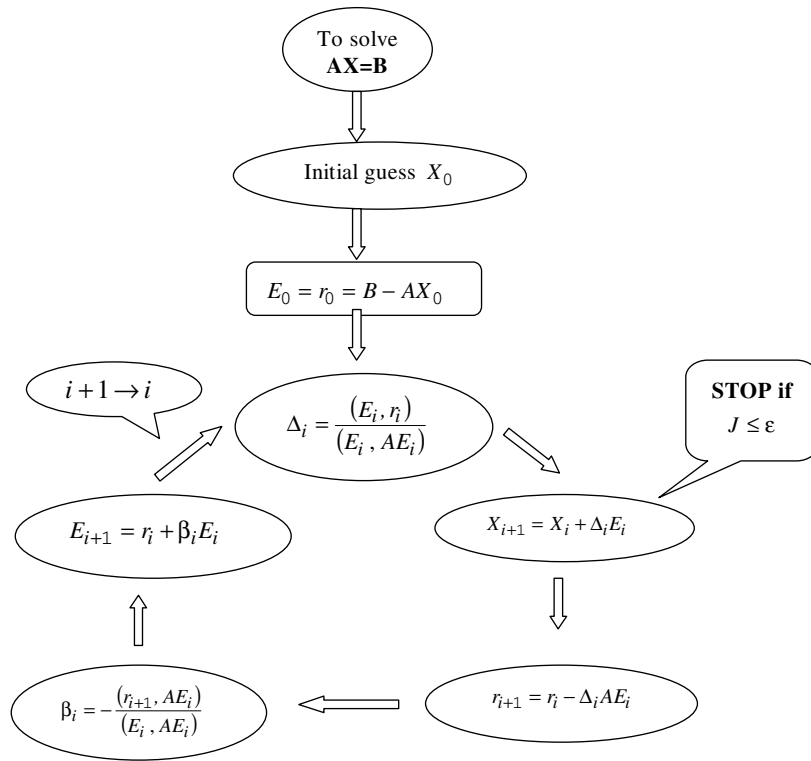


Figure 2 : Numerical procedure for the iterative conjugate gradient method.

If measurement error is to be considered, according to Alifanov(1974), the stress measurement residual can be written as

$$\sigma_{xx,estimated} - \sigma_{xx,measured} \approx \Delta_1 \tag{28}$$

$$\sigma_{xy,estimated} - \sigma_{xy,measured} \approx \Delta_2 \tag{29}$$

and

$$\sigma_{yy,estimated} - \sigma_{yy,measured} \approx \Delta_3 \tag{30}$$

where Δ_1 , Δ_2 and Δ_3 are the standard deviation of the stress measurement errors in the normal or in the shear direction. Substituting (28), (29) and (30) into equation (20), and assuming that all of Δ s are constants, the following expression for ϵ is obtained,

$$\epsilon = N (\Delta_1^2 + \Delta_2^2 + \Delta_3^2) . \tag{31}$$

It is obviously from the above equation that the convergent criterion is directly dependent of the number of sensors, N being selected. Similarly, the stopping criterion for the case of displacement measurement error can also be obtained.

6 Numerical Results and Discussions

We discuss the problem of an elastic media under various loading condition. The Young's modulus is assumed to be 50MPa at first, and the Poisson ratio is 0.3. The crack is assumed to be 2/3m long, which is about 6.7 % of the edge of the 10m by 10m square plate. The inverse problem is to determine the loading condition on boundary CD using the internal measurements. The boundary AB is fixed throughout the analysis, and the rest of the boundaries are traction free. The entire boundaries are modeled by 40 evenly distributed continuous quadratic boundary elements, while the crack is divided into seven uneven sized, discontinuous *displacement discontinuity quadratic boundary elements*. Sensor points are positioned parallel to the boundary AB, and at various locations from the base line AB.

Case 1: Uniform tension condition, i.e., $t_y=50MPa$ on boundary CD

When the conjugate gradient method being applied to the problem, the constant of ϵ has to be small enough to give accurate result. At the early stage of the numerical ex-

periment, equation (16) or (21) was used, and a scaling factor of $O(\mu)$ was used within the numerical program while solving the problem. However, when the material constant of steel is used, the result is getting worse, Fig. 3. This is due to the inconsistency of the order of magnitude with respect to μ in the sensitivity matrices H 's and G 's as described in previous section. Therefore, equation (22) and (23) are adopted for the remaining numerical experiments.

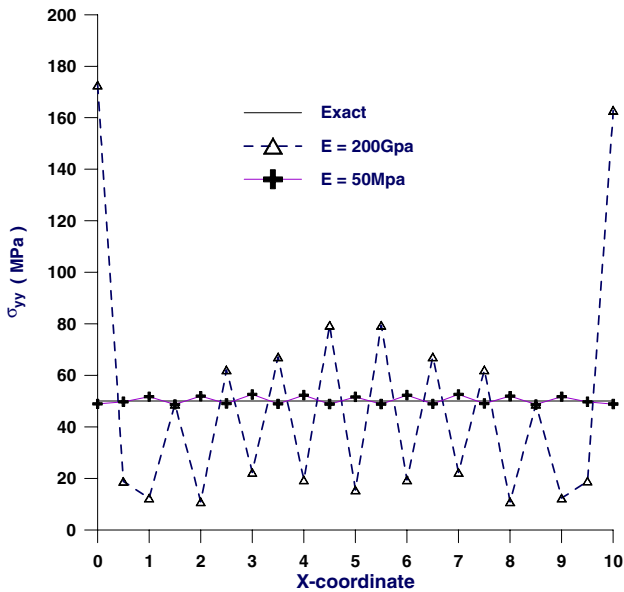


Figure 3 : The unknown traction solved by the conjugate gradient method, using 21 *stress* measurement data and showing the difference due to the change of material constant. Sensor's location is at $y=9.7m$, and the crack is at $y=5.0$

While using the regularization method, determination of the regularization parameter, α is important in order to reach an acceptable result. The regularization parameter has to be large enough in order to smooth the singular matrix, $\mathbf{A}^T \mathbf{A}$, and it also needs to be small enough in order not to alter the solution. Fig. 4 shows the results by using different value of the regularization parameters. If the regularization parameter is too small, the inverse solution is either unsolvable or unacceptable. If α is too big (for example $\alpha=1$ and not showing in the figure), the smoothing result by no mean is close to the exact solution.

According to Fig. 5 and 6 that the inverse analysis seems not very sensitive to a wide range selection of α . Then, it

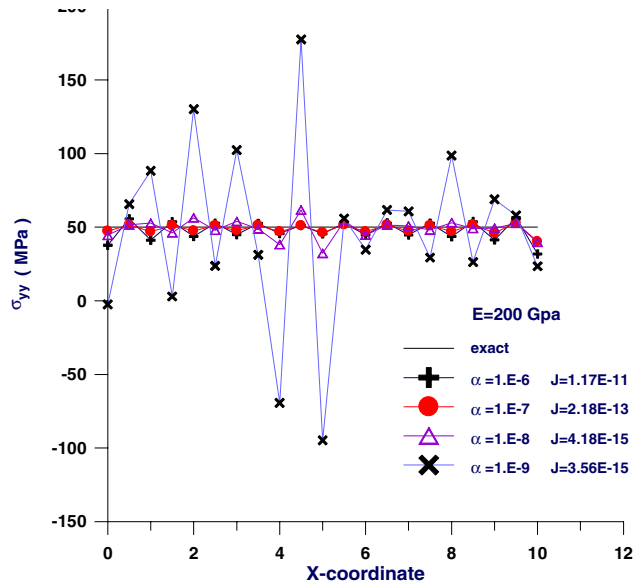


Figure 4 : The unknown traction solved by the regularization method with various α using 21 *displacement* measurement data. Sensor's location is at $y=9.7m$, and the crack is at $y=5.0$

is possible to guess an optimum value of α beforehand to solve the inverse problem by the regularization method. It can be seen from all of the above figures that the inverse analysis using stress measurement gives better results than using the displacement measurement, and the reason for this is still unclear.

Case 2: Various loading condition on the boundary CD

From previous examples, we have found that introducing the scaling factor in (22) and (23) has a greater benefit for the numerical calculation, especially for the iterative conjugate gradient method. It gives a quicker and a more stable convergent result. For the regularization method, a one-shot estimation of the regularization parameter is possible to get an accurate inverse solution. Different loading conditions on CD are also tested in order to confirm the feasibility of the proposed inverse numerical procedure. Fig. 7 gives the result of a triangle-type of boundary loading by either the stress or the displacement data. If the boundary loading with suddenly jump and the in-plane bending condition are also considered, and we are happy with the results given by the conjugate gradient method or by the regularization method, see Fig 8. and Fig. 9.

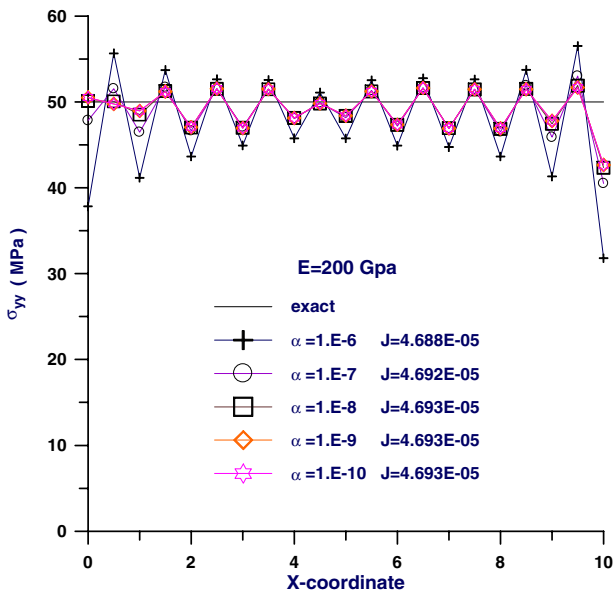


Figure 5 : The unknown traction solved by the regularization method with various α using 21 *displacement* measurement data–A scaling factor is introduced. Sensor’s location is at $y=9.7\text{m}$ and the crack is at $y=5.0\text{m}$.

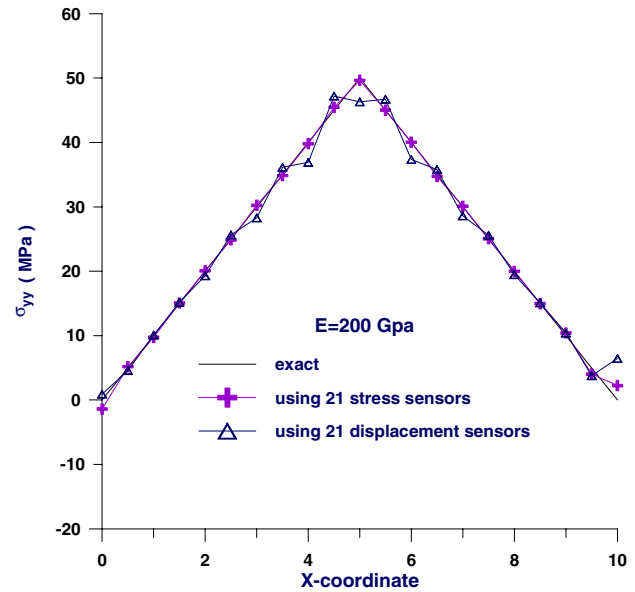


Figure 7 : The unknown traction solved by the regularization method for $\alpha=10^{-9}$ –A scaling factor is introduced. Sensor’s location is at $y=9.7\text{m}$, and the crack is at $y=5.0$

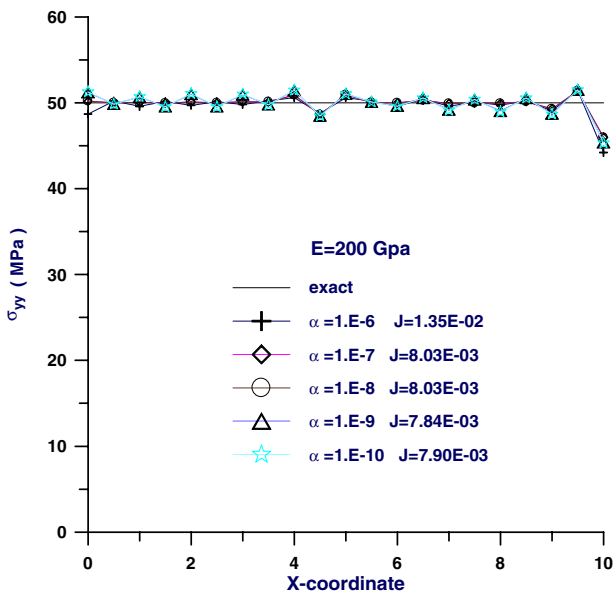


Figure 6 : The unknown traction solved by the regularization method with various α using the 21 *stress* measurement data–A scaling factor is introduced. Sensor’s location is at $y=9.7\text{m}$, and the crack is at $y=5.0$

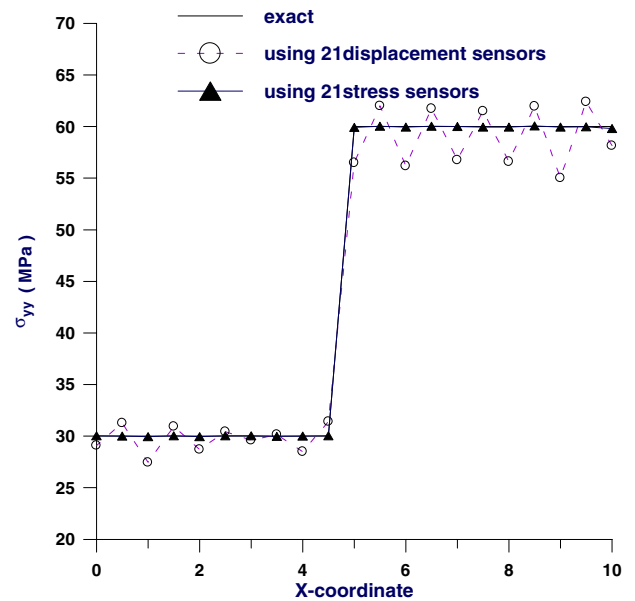


Figure 8 : The non-uniform unknown traction solved by the conjugate gradient method–A scaling factor is introduced. Sensor’s location is at $y=9.7\text{m}$, and the crack is at $y=5.0$

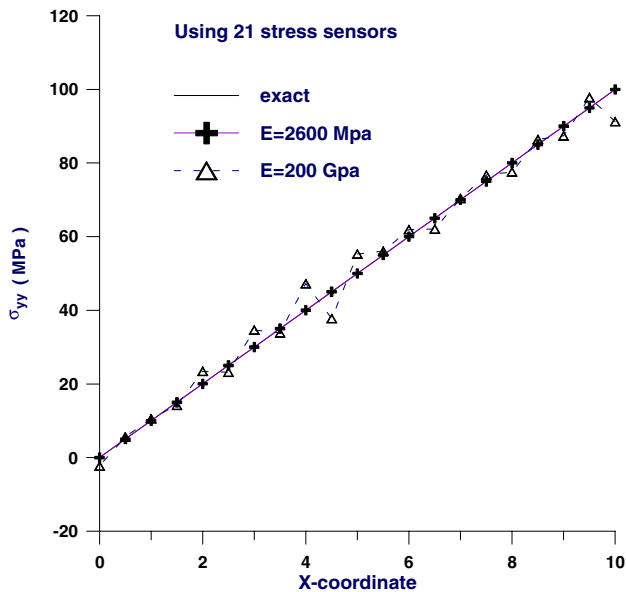


Figure 9 : The unknown traction solved by the regularization method for $\alpha=10^{-9}$ (in-plane bending condition)—A scaling factor is introduced. Sensor’s location is at $y=9.7\text{m}$, and the crack is at $y=5.0$

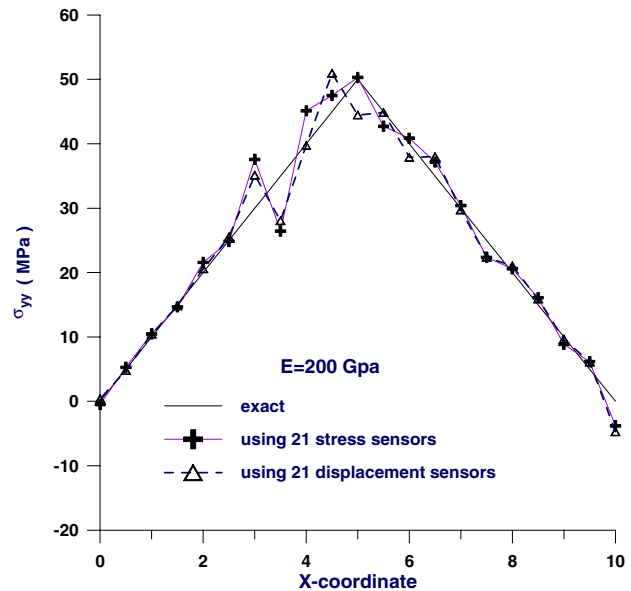


Figure 10 : The inverse analysis for the crack locating at $y=7.5$ and the sensors being at $y=9.7$, using the regularization method and $\alpha=10^{-9}$. (cf. Fig. 8)

Case 3: Influence of crack size, relative distance between crack and sensors

The distance between the crack and the sensor points also plays a certain role for the inverse analysis. We now move the crack closer to the boundary and compare the result with previous case. It is found that the solution solved by the proposed numerical procedure is still very accurate, except for one boundary element near the central region of the previous example, comparing Fig. 7 with Fig.10. If the sensors move away from the boundary, and the crack moves even closer to the sensors, the predicted boundary traction is almost identical to the exact solution if the stress sensors are used, see Fig. 11. The above two numerical studies show that the location of the crack and the sensors do not have much influence on the inverse analysis. However, the type of measuring sensor will make a difference on the final result. According to our numerical experiment, even though a larger crack is considered, the inverse solution by the proposed technique is still very accurate.

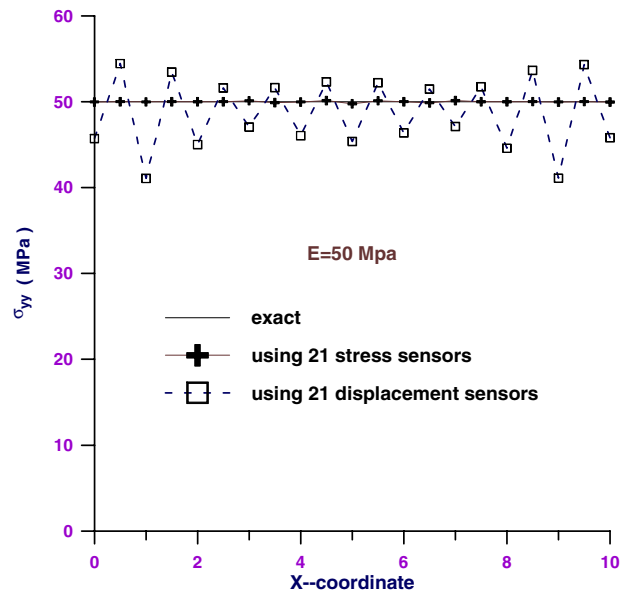


Figure 11 : The sensitivity analysis by changing the crack locating to $y=9.0$ and the sensors to $y=9.4$, using the regularization method and $\alpha=10^{-9}$

Case 4: The Measurement Error

When performing the experiment, one will have to deal with the measurement error. There is no exception for the inverse problem. All of the previous cases we have studied are mainly for testing the numerical procedure. Let's now consider the following case: the Young's modulus is 200Gpa and the displacement sensors are used as the measuring device. If we consider the measurement error distribution as stated in previous section, and the standard deviation for measuring error, $\bar{\sigma}$ being 1% of the averaging measurement. The inverse calculation shown in Fig. 12 states that the inverse solution seems very sensitive to the measurement error. Sometimes, when the displacement measurement data being used for the inverse analysis, the predicted boundary traction is not very good. However, when the stress measurement data being used, the predicted boundary information either by the conjugate gradient method, Fig.13, or by the regularization method, Fig. 14, with measurement error is pretty close to the exact solution.

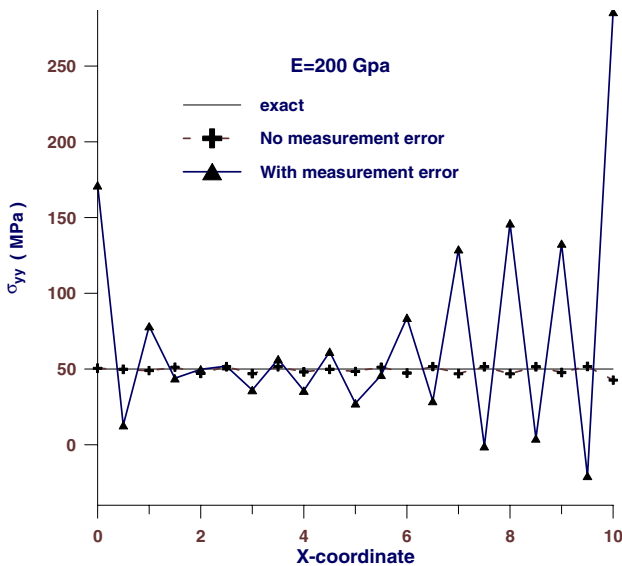


Figure 12 : The influence of the *displacement* measurement error on the inverse solution with 99% of confidence solving by the regularization method with $\alpha=10^{-9}$. The standard deviation of measurement error is taken as 1 percent of the average measurement, and 21 sensors are used.

To reduce the number of the sensors, we can use a coarser mesh on the boundary. Let's assume only five boundary

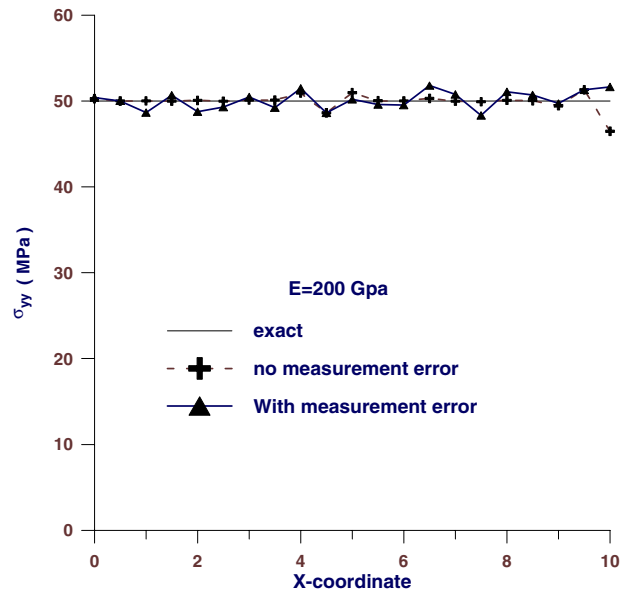


Figure 13 : The influence of the *stress* measurement error on the inverse solution with 99% of confidence solving by the conjugate gradient method. The standard deviation of measurement error is taken as 1 percent of the average measurement, and 21 sensors are used.

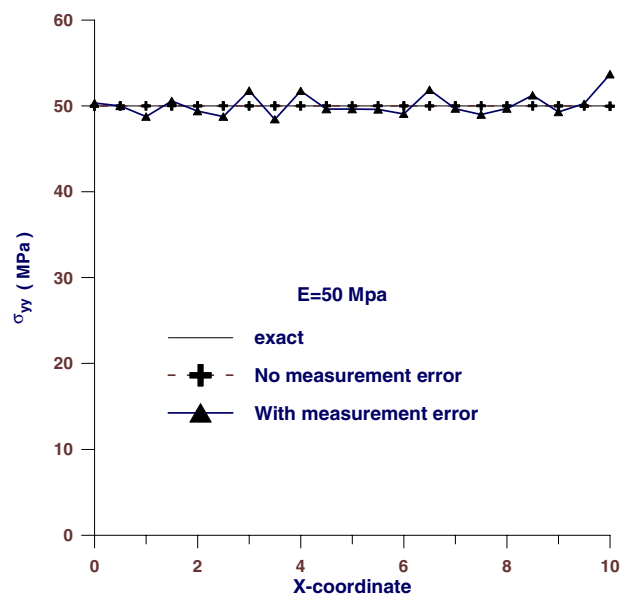


Figure 14 : The influence of the *stress* measurement error on the inverse solution with 99% of confidence solving by the regularization method with $\alpha=10^{-9}$. The standard deviation of measurement error is taken as 1 percent of the average measurement, and 21 sensors are used.

elements on the unknown traction boundary. That is, the number of unknown is reduced by nearly 50 percents. It can be seen from Fig. 15 that the accuracy is still very good if compared with previous calculation. Changing the sensors' location, Fig. 16 will have small effect on the final result.

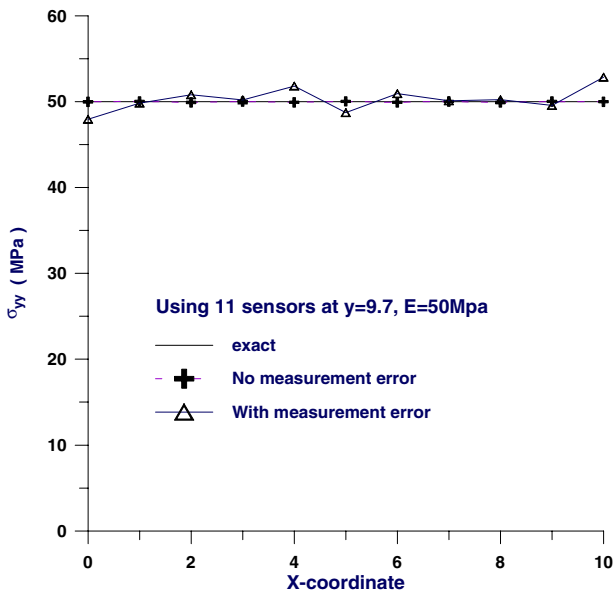


Figure 15 : The influence of the measurement error with 99% of confidence solving by the regularization method with $\alpha=10^{-6}$. Stress sensor locating at $y=9.7$ and the crack being at $y=5.0$; the Young's modulus $E=50\text{Mpa}$

When measurement error being considered, equation (24) poses the stopping criterion for the numerical calculation. For the regularization method, the functional J in general will satisfy the stopping criterion of (24). However, when the conjugate gradient method is used, it will result in a less accurate convergent result. If more iteration steps are calculated, a better solution can be reached, see Fig. 17.

7 Conclusion

A scaling factor is introduced into the displacement and the traction boundary integral equations while solving the inverse problem in consideration. All of our numerical experiments show that when the stress measuring data being used in the inverse analysis, the predicted boundary traction is more accurate than those by using the displacement measurement, and the theoretical base for this is unclear and still needs further study.

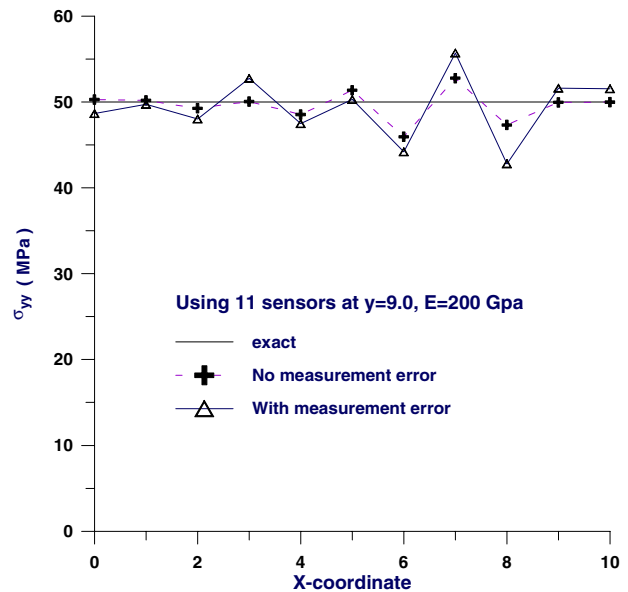


Figure 16 : The influence of the measurement error with 99% of confidence solving by the regularization method with $\alpha=10^{-6}$. Stress sensor locating at $y=9.0$ and the crack being at $y=5.0$; the Young's modulus $E=200\text{Gpa}$

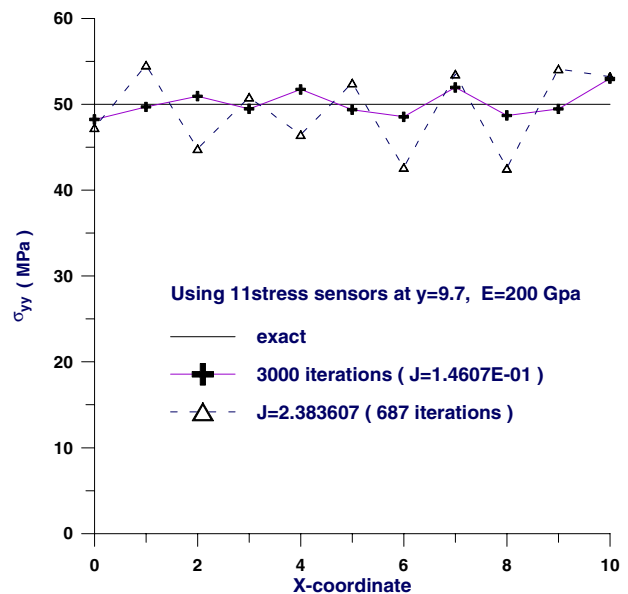


Figure 17 : The inverse analysis using the conjugate gradient method and showing the result from different convergent criteria. Only 11 stress sensors are used and $\epsilon=2.497384$. Sensor locating at $y=9.7$ and the crack being at $y=5.0$; the Young's modulus $E=200\text{Gpa}$

When the sensors being too far away from the boundary, the inverse result for the boundary traction is less accurate. Once we move the sensors closer to the boundary, the estimated boundary traction is getting better. This is because that the sensitivity matrix, $\mathbf{A}^T\mathbf{A}$ in equation (18) is more and more ill-conditioned as the distance between sensors and boundary is increased.

Comparing the conjugate gradient method to the regularization method, it is found that the later will be much more effective than the former. By using the regularization method, the choice of the regularization is basically by try and error. However, if the regularization parameter falls within the range $(10^{-4}, 10^{-9})$, it will give pretty good prediction of the unknown boundary traction. Thus, there is no need to find an optimum value of the regularization parameter for the best inverse solution, and a one-shot regularization solution is good enough for the final solution. When the first order regularization square matrix is used, there is no sign of improvement for the inverse solution. Besides that, when considering the measurement error and using the Alifanov(1974) convergent criterion, the one-shot regularization method will satisfy the convergent requirements posed by (24) and (31). However, when the conjugate gradient method is used, equation (31) will result in a less accurate convergent result. More iteration steps are required to get a better solution.

Finally, we would like to comment on our works with Huang and Shih(1997). From Fig. 12, we can see that the displacement measurement error is more sensitive to the solution if a crack is considered in the inverse analysis. Neglecting the existence of a small crack, the inverse solution will most likely mislead the real boundary loading condition, see Fig. 18.

Acknowledgement: The authors would like to thank Professor C.H. Huang for his useful discussions. The support by the National Science Council under project NSC-89-2611-E-006-028 is also acknowledged

References

Alifanov, O.M.(1974): Solution of an inverse problem of heat conduction by iteration methods, *J. of Engineering Physics*, 26, pp.471-476.

Becker, A. A.(1992): *The boundary element Method in Engineering*, McGRAW-HILL.

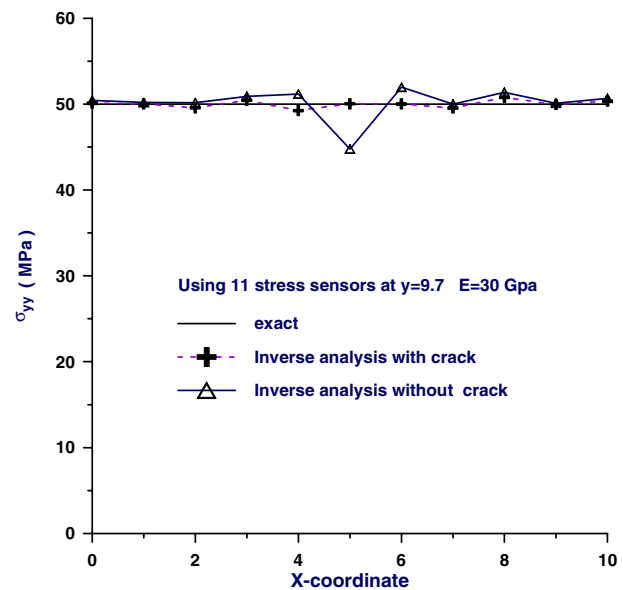


Figure 18 : The inverse analysis using the regularization method with or without considering the existence of a small crack. 11 stress sensor locating at $y=9.7$ and the crack being at $y=9.0$.

Brebbia C. A. and Dominguez J.(1992): *Boundary Elements, An Introductory Course.*, 2nd Edition, Computational Mechanics Publications.

Chen, J. T. and H. K. Hong,(1999): Review of dual boundary element methods with emphasis on hypersingular integrals and divergent series, *Applied Mechanics Reviews*, ASME, Vol. 52, No.1, pp.17-33.

Gao, Z. and Mura, T.(1989): Inversion of residual stresses from surface displacements", *J. Appl. Mech*, *ASME Trans.*, 54, pp.508-513.

Hong, H. K. and Chen, J. T.(1988): Generality and special cases of dual integral equations of elasticity, *Journal of the Chinese Society of Mechanical Engineers*, Vol.9, No.1, pp.1-9.

Hong, H.K. and Chen, J.T.(1988) Derivations of integral equations of elasticity, *J. Eng. Mech.*, *ASCE*, 114, No.6, pp.1028-1044.

Huang, C. H. and Shih, W. Y.(1997): A boundary Element based solution of an inverse elasticity problem by conjugate gradient and regularization method, *Inverse problems in engineering*, 4, pp.295-321.

Huang, C.H. and Shih, W.Y.(1999): An inverse problem in estimating interfacial cracks in bimetals by boundary element technique”, *Int. J. Numer. Meth. Engng.*, 45, 1547-1567.

Ingham, D. B. and Wrobel, L. C.(1997): Boundary integral formulations for Inverse Analysis, CMP, UK.

Kammerer, W.J. and Nashed, M.Z.(1972): On the convergence of the conjugate gradient method for singular linear operator equations, *SIAM J. Numer. Analysis*, 9 (1) pp.165-181.

Koya, T., Yeih, W. and Mura, T.(1993): An inverse problem in elasticity with partially over-prescribed boundary conditions, part II: Numerical results and examples, *J. Appl. Mech. ASME Trans*, 60, pp. 601-606.

Kubo, S.(1988): Inverse problems related to the mechanics and fracture of solids and structures, *JSME International Journal*, Vol.31, pp.157-166.

Maniatty, A. and Zabaras, N.(1994): Investigation of regularization parameters and error estimating in inverse elasticity problem, *Int. J. Numer. Meth. Eng.*, 37, pp.1039-1052.

Mellings, S. C. and Aliabadi, M. H.(1995): Flaw identification using the boundary element method, *Int. J. Num. Meth, Engng.*, 38, pp. 399-419.

Mi Yaoming(1996): *Three-Dimensional Analysis of Crack Growth*, Computational Mechanics Publications, Southampton, U. K.

Pasquetti, R and Petit, D.(1995): Inverse Diffusion by Boundary elements, *Engineering Analysis with Boundary Elements*, 15, pp.197-205.

Portela, A. and Aliabadi, M. H.(1992): The dual boundary element method: Effective implementation for crack problem, *Int. J. Numer. Meth. Engng.*, 33, pp.1269-1287.

Portela, A.(1993): *Dual boundary element analysis of crack growth*, Topics in Engineering.14, CMP, UK.

Yeih, W., Koya, T. and Mura, T.(1993): An inverse problem in elasticity with partially over-prescribed boundary conditions, part I: Theoretical approach”, *J. Appl. Mech. ASME Trans.*, 60, pp. 595-600,.

